

## Upstream stagnation points in stratified flow past obstacles

Peter G. Baines<sup>a</sup> and Ronald B. Smith<sup>b</sup>

<sup>a</sup> CSIRO Division of Atmospheric Research, Aspendale, Vic. 3195, Australia

<sup>b</sup> Department of Geology and Geophysics, Yale University, New Haven, CT 06511, USA

(Received 23 July 1991; revised 10 August 1992; accepted 2 September 1992)

### ABSTRACT

Baines, P.G. and Smith, R.B., 1993. Upstream stagnation points in stratified flow past obstacles. *Dyn. Atmos. Oceans*, 18: 105–113.

An experimental study has been made of stagnation points and flow splitting on the upstream side of obstacles in uniformly stratified flow. A range from small to large values of  $Nh_m/U$  (where  $N$  is the buoyancy frequency,  $h_m$  is the maximum obstacle height and  $U$  is the undisturbed fluid velocity) has been covered, for three obstacle shapes which are, respectively, axisymmetric, and elongated in the across-stream and in the downstream directions. Upstream stagnation for the first two of these models does not occur until  $Nh_m/U > 1.05$ , where it occurs at  $z \approx h_m/2$ . On the central line below this point the flow descends and diverges, and we term this 'flow splitting'. For the third model (elongated in the downstream direction), upstream stagnation first occurs at  $Nh_m/U \approx 1.43$ , at  $z \approx 0$ . Results for this obstacle are not consistent with the 'Sheppard criterion', and this upstream flow stagnation is not apparently related to lee wave overturning, in contrast to flow over two-dimensional obstacles.

### 1. INTRODUCTION

Stagnation of stratified flow on the upstream side of an obstacle is dependent on the overall obstacle shape, among other factors. Even for a very broad three-dimensional obstacle, the initially two-dimensional flow in the central region of the obstacle will eventually adjust to the three-dimensionality and the presence of ends through signal transport by internal wave propagation, and the final steady state will be very different in consequence (Baines, 1990). This paper examines the nature of upstream flow splitting and stagnation, and the effect of obstacle shape.

Linearised theory of uniformly stratified flow past three-dimensional obstacles indicates that, for sufficiently large  $Nh_m/U$  (where  $N$  is the

---

Correspondence to: P.G. Baines, CSIRO Division of Atmospheric Research, Aspendale, Vic. 3195, Australia.

buoyancy frequency,  $h_m$  is the maximum obstacle height and  $U$  is the undisturbed fluid velocity), the flow may become stagnant in two regions (Smith, 1989). The first of these is in the lee wave field as described by, for example, Huppert and Miles (1969), and is associated with lee wave breaking and overturning. The second possible stagnation region is on the forward face of the obstacle, and occurs because the oncoming flow at ground level encounters an adverse pressure gradient which reduces its speed. As  $Nh_m/U$  increases, stagnation may appear first in either of these regions, depending on the obstacle shape. If  $a$  is the obstacle half-width in the downstream direction and  $b$  the half-width in the across-stream direction, Smith (1989) suggested that stagnation occurs first on the forward face if  $a/b > 1$ , and first in the lee wave field if  $a/b < 1$ . Furthermore, stagnation on the forward face is associated with flow splitting at low levels. Fluid encountering a localised region of increasing pressure may be pushed sideways, so that the fluid flows around the obstacle rather than over it. This results in reduced amplitude of disturbances aloft, so that stagnation and wave breaking may not occur there at all.

The question of whether fluid flows around or over a three-dimensional obstacle has frequently been described in terms of the Sheppard criterion (e.g. Snyder et al., 1985), which hypothesises that fluid approaching an obstacle on the centre-line will surmount the obstacle if it has enough kinetic energy to overcome the potential energy embodied in the mean stratification. For uniform  $U$  and  $N$ , this implies that the fluid can rise a height  $U/N$  above its upstream level, but no further. This criterion is consistent with many experimental results (Snyder et al., 1980, 1985) for nearly axisymmetric obstacles, and obstacles elongated in the across-stream direction. However, it has no theoretical foundation, as the simple energy argument from which it is derived omits the effect of the perturbation pressure gradient in the fluid, and this is of the same magnitude as the other terms in the equation (Smith, 1989).

To investigate the behaviour of the upstream stagnation points, and the associated relevance of the 'Sheppard criterion', the laboratory experiments described here were undertaken to examine the flow on the surface of a range of obstacles with  $a/b > 1$ ,  $a/b = 1$  and  $a/b < 1$ . In fact, the leading face of an obstacle placed on a plane surface must have (at least) two stagnation points if it has any at all (Hunt et al., 1978). Figure 1 (from Hunt and Snyder, 1980) shows schematically the observed stagnation points on an axisymmetric hill for  $Nh_m/U = 2.5$ . The lower stagnation point,  $P_1$ , is associated with a small degree of overturning; it occurs at the lowest levels of the obstacle, or even upstream of it, and the local lifting of the fluid has been associated with the formation of cloud lines upstream of Hawaii (Smolarkiewicz et al., 1988). However, these details do not concern us here.

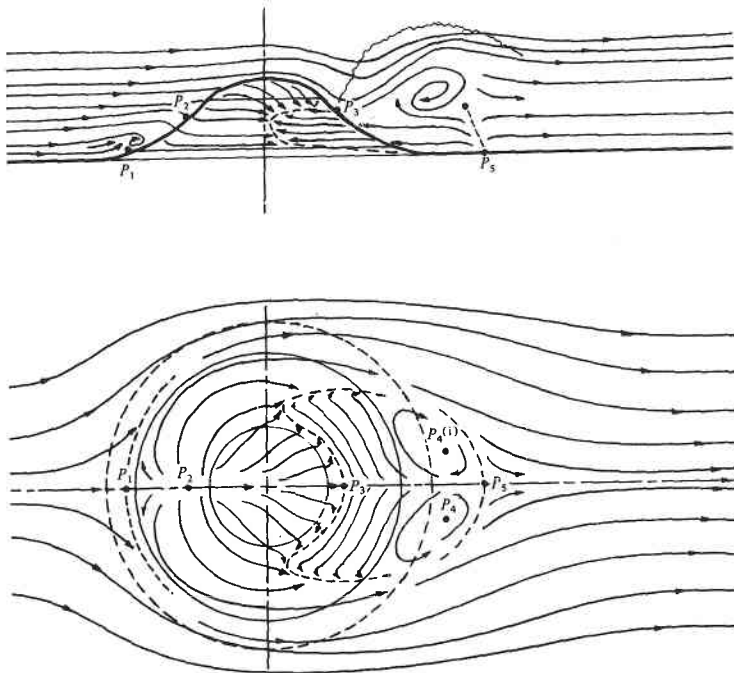


Fig. 1. A sketch of observed streamlines from an experiment with uniformly stratified flow past an axisymmetric hill, showing flow on the central plane and on the obstacle surface for  $Nh_m/U = 2.5$  (Hunt and Snyder, 1980; reproduced with the permission of Cambridge University Press).

The second stagnation point,  $P_2$ , occurs much higher, and is the principal point of interest in this study.

## 2. THE EXPERIMENT

Four obstacles that have the form

$$h(x, y) = \frac{h_1}{\left[1 + \left(\frac{x}{a}\right)^2 + \left(\frac{y}{b}\right)^2\right]^{3/2}} - h_2 \quad (1)$$

where  $h > 0$ , with  $h = 0$  otherwise, were machined from solid Perspex using an automated milling machine. The values of  $h_1$ ,  $h_2$ ,  $a$  and  $b$  are given in Table 1. For each experimental run, one of these obstacles was placed on a tray (thickness 2 mm) that was towed at uniform speed through a tank of uniformly stratified fluid. The obstacles were situated approximately 30 cm downstream from the leading edge of the tray. Stratification was achieved with salt water, by the usual two-tank mixing process. The tank used had

TABLE 1

Values of the model parameters used in the experiments

Model no.	$a$ (cm)	$b$ (cm)	$h_1$ (cm)	$h_2$ (cm)	$h_m = h_1 - h_2$
1	13.1	4.2	6.49	1.49	5.0
2	11.2	4.2	5.525	1.275	4.25
3	11.2	11.2	5.525	1.275	4.25
4	11.2	22.4	5.525	1.275	4.25

2.26 m length, 1.13 m width, and 0.23 m depth, and was filled to a depth of 0.18 m. As may be seen from Table 1, this depth is about four times the height of the topography  $h_m$ , and for these three-dimensional shapes the flow at low levels (which is the primary concern here) should differ by an insignificant amount from the flow with infinite depth. We are also concerned primarily with flows where  $Nh_m/U > 1$ , and Table 1 shows that this implies that  $Na/U \geq 3$  for all cases, so that the flow is approximately hydrostatic. It should be noted that obstacles 2, 3 and 4 all have the same cross-section along the  $x$ -axis, so that differences in the flow are solely due to the variation in  $b$ . In these experiments  $N \approx 1.3$  rad/s, so that, for  $Nh_m/U = 2$ ,  $U \approx 3$  cm/s and the Reynolds number  $Re \approx 1300$ . Hence the Reynolds number is large for all situations of interest, and the dependence of the flow properties on  $Re$  should be small.

Flow patterns on the surface were visualised by potassium permanganate dye from pellets that were sprinkled over the obstacle to give adequate coverage. The dye is slightly denser than fresh water, and in consequence has a slight tendency to sink. This property was tested with tows using fresh water alone, and the variation in flow patterns on the forward face of the obstacle with the obstacle speed allowed this effect to be estimated. It may be minimised in three ways: (1) by maximising the stratification, so that buoyancy caused by salt stratification minimises the effect of buoyancy of the dye; (2) maximising the towing speed; (3) by using small dye pellets. As the principal objective of the experiment was to determine the upstream stagnation points, these considerations are important, and these factors were carefully monitored to achieve repeatable and reliable results. A succession of plan-view photographs of the dye patterns were taken after the obstacle had travelled a distance of several times its downstream length, and the similarity between these successive frames showed that steady state in the flow had been realised.

Flow patterns on the vertical central plane of the obstacle were also observed. This was done by adding a suitable number of small (diameter 0.2 mm) polystyrene beads to the fluid, and illuminating this section by a vertical sheet of laser light. The beads then become streaks showing the

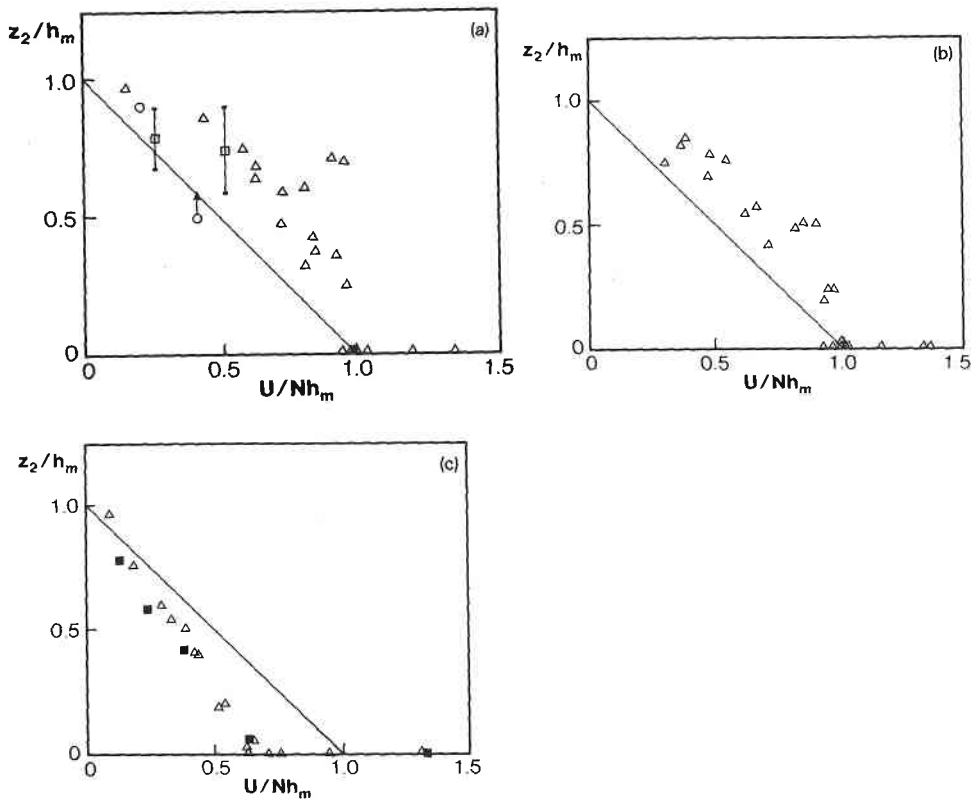


Fig. 2. Observed heights  $z_2$  of the separation point  $P_2$  on the upstream face of the obstacle, as functions of  $Nh_m/U$ . The straight line has been drawn for comparison purposes only. (a) model 3 ( $\Delta$ ) (Table 1), with additional results from Hunt and Snyder (1980) ( $\circ$ ) and Hanazaki (1988, numerical) ( $\square$ ). (b) Model 4. (c) Model 1 ( $\Delta$ ) and model 2 ( $\blacksquare$ ). Points on the line  $z_2 = 0$  indicate that no stagnation point was seen in that experiment.

velocity field in time-exposure photographs of this vertical plane. The development of the motion with time was then recorded on videotape from a moving camera, for values of  $Nh_m/U$  covering the same range as for the dye experiments.

### 3. RESULTS

The results of about 75 tows with the four obstacles are shown in Fig. 2. Fig. 2(a) shows the height  $z_2$  of the stagnation points  $P_2$  for the axisymmetric obstacle (model 3) as a function of  $Nh_m/U$ , together with some results inferred from Fig. 15 of Hunt and Snyder (1980) (of which Fig. 1 here is an example), and from the numerical computations of Hanazaki (1988) for flow past a sphere. These show that, for  $Nh_m/U < 1.05$ , there is no

stagnation on the forward face for these smooth obstacles (the sphere is not smooth in the same sense as the other shapes, and it always has a stagnation point at  $x = 0$ ; however, the results for  $z_2$  are consistent, as shown). Further, for  $Nh_m/U \approx 1.05$ , stagnation occurs at a height  $z_2$  of about  $0.5h_m$ , and the flow is split about the vertical plane of symmetry at all heights below this, because the lower separation point  $P_1$  is at a very low or even zero altitude  $z_1$ . This flow splitting is marked by the observed property that fluid leaving the centre plane near the obstacle surface descends and divides for  $z$  below  $z_2$ . For  $z$  above  $z_2$  it rises, as an undivided continuous sheet on the surface of the obstacle.

The initial appearance of stagnation at  $z \approx h_m/2$  is consistent with the linear solutions for the pressure field on the forward face (Smith, 1980; Phillips, 1984), where the maximum of the surface pressure occurs at about this height (although there is some dependence on obstacle shape). When flow splitting first occurs,  $P_1$  should be very close to  $P_2$ , but these observations show that the range of  $Nh_m/U$  for which this occurs must be very small, and as  $Nh_m/U$  increases  $P_1$  (and  $z_1$ ) must descend very quickly to very low or zero altitude, with descending flow and flow splitting occurring in between. As  $Nh_m/U$  increases further,  $P_2$  moves higher, and  $z_2$  approaches  $h_m$  as  $U/Nh_m$  approaches zero. These heights are all significantly above the expected upstream heights  $z_s$  of the central separation or 'dividing' streamline that intersects  $P_2$ , which for these axisymmetric obstacles have been reported (Snyder et al., 1980, 1985, Hanazaki, 1988) to be consistent with the 'Sheppard criterion'

$$z_s/h_m = 1 - U/Nh_m \quad (2)$$

In experiments with the axisymmetric obstacle (model 3), the lee waves were observed to become steep in the range  $1 < Nh_m/U < 2$ , but not so steep as to produce wave overturning and stagnation in the lee wave field. In fact, the latter were never observed, either in the steady state or in the temporal development of the flow when towing is commenced suddenly from a state of rest, for any value of  $Nh_m/U$ . This appears to be consistent with the results presented by both Hunt and Snyder (1980) and Hanazaki (1988), for various axisymmetric obstacle shapes (the overturning depicted in the wake region of Fig. 1 was not conspicuous in the present experiments, and is not related to breaking lee waves). The reason for this lack of overturning, regardless of the value of  $Nh_m/U$ , may be attributed to the upstream flow splitting, which reduces the effective obstacle height, as far as the lee waves are concerned (although non-hydrostatic and viscous effects may also have a small influence). The onset of this flow splitting is related to the pressure maximum on the forward face, which is related to the total drag, but this does not necessarily imply or relate to lee wave

breaking, so that it appears that upstream flow splitting and lee wave overturning are unrelated phenomena. Upstream flow splitting is, however, clearly related to lee-side eddy formation, as the nearly horizontal flow around the obstacle is subject to the familiar process of boundary-layer separation, producing a wake that is analogous to that formed by two-dimensional flow past a cylinder.

The height  $z_2$  of the separation point  $P_2$  for model 4 (wide in the across-stream direction) is shown in Fig. 2(b). The variation of  $z_2$  with  $Nh_m/U$  is very similar to that for the axisymmetric obstacles, and has a comparable degree of scatter in the data. Upstream flow splitting commences when  $Nh_m/U$  rises above 1.05, and the depth range over which it occurs increases rapidly to be  $0 < z < 0.5h_m$ .  $z_2$  then rises toward  $h_m$  as  $Nh_m/U$  increases.

The height of separation point  $P_2$  for models 1 and 2 (narrow in the across-stream direction) is shown in Fig. 2(c). There is no significant difference between the results for these slightly different shapes. Here there is no upstream stagnation for  $U/Nh_m > 0.7$  ( $Nh_m/U < 1.43$ ), and  $z_2$  increases linearly as  $U/Nh_m$  decreases below this value.  $z_1$  is effectively zero in this case, so that the flow splitting region (with flow descending rather than ascending on the centreline) grows upward from the base level. These results are contrary to the Sheppard criterion (eqn. (2)), as fluid on the centreline at ground level can pass over the top of the obstacle if  $Nh_m/U \leq 1.43$ , although the divergence of the flow along this centre streamline is fairly large. The result is that the quantity of fluid following this path is very small. This demonstrates that the Sheppard criterion is not empirically valid for all obstacle shapes, although it should be useful as a working guide for most practical purposes.

#### 4. CONCLUSIONS AND INFERENCES

Our conclusions are based on inferences from the experiments with the smooth models of Table 1, with the results given in Fig. 2, and are as follows:

(1) Smooth symmetrical obstacles which are axisymmetric, or wider in the across-stream direction than in the downstream direction, have no stagnation points on the forward face if  $Nh_m/U < 1.05$ . If  $Nh_m/U$  is increased to just above this value, flow splitting (with downward motion on the centreline) occurs below a height  $z_2 \approx h_m/2$ . If  $Nh_m/U$  is increased further, the stagnation point at the top of the flow splitting region moves toward the top of the obstacle. There was no significant detectable difference in this behaviour between models 3 and 4. The apparent discontinuous change in the nature of the flow on the windward slope near  $Nh_m/U =$

- Phillips, D.S., 1984. Analytical surface pressure and drag for linear hydrostatic flow over three-dimensional elliptical mountains. *J. Atmos. Sci.*, 41: 1073-1084.
- Smith, R.B., 1980. Linear theory of stratified hydrostatic flow past an isolated mountain. *Tellus*, 32: 348-364.
- Smith, R.B., 1989. Mountain-induced stagnation points in hydrostatic flow. *Tellus*, 41A: 270-274.
- Smolarkiewicz, P.K., Rasmussen, R.M. and Clark, T.L., 1988. On the dynamics of Hawaiian cloud bands: island forcing. *J. Atmos. Sci.*, 45: 1872-1905.
- Snyder, W.H., Britter, R.E. and Hunt, J.C.R., 1980. A fluid modelling study of the flow structure and plume impingement on a three-dimensional hill in stably stratified flow. In: J.E. Cermak (Editor), *Proc. 5th Int. Conf. on Wind Eng.*, July 1979, Fort Collins, CO, Vol. 1, Pergamon, Oxford, pp. 319-329.
- Snyder, W.H., Thompson, R.S., Eskridge, R.E., Lawson, R.E., Castro, I.P., Lee, J.T., Hunt, J.C.R. and Ogawa, Y., 1985. The structure of strongly stratified flow over hills: dividing streamline concept. *J. Fluid Mech.*, 152: 249-288.